

# Vision-Based Structural Identification Using an Enhanced Phase-Based Method <sup>†</sup>

Samira Azizi <sup>1,\*</sup>, Kaveh Karami <sup>2</sup> and Stefano Mariani <sup>1</sup>

<sup>1</sup> Department of Civil and Environmental Engineering, Politecnico di Milano, Milano, Italy; stefano.mariani@polimi.it

<sup>2</sup> Department of Civil Engineering, University of Kurdistan, Sanandaj, Iran; ka.karami@uok.ac.ir

\* Correspondence: samira.azizi@mail.polimi.it

<sup>†</sup> Presented at the 10th International Electronic Conference on Sensors and Applications (ECSA-10), 15–30 November 2023; Available online: <https://ecsa-10.sciforum.net/>.

**Abstract:** Operational modal analysis is based on data collected with a network of sensors installed on the monitored structure, to measure its response to the external stimuli. As the instrumentation can be costly, sensors get located at a limited number of spots where damage-sensitive features can be hopefully sensed. Hence, the actual capability to detect in real time a drift from the undamaged structural state might get detrimentally affected. Non-contact measurement methods resting on e.g., digital video cameras, which have gained interest in recent years, can instead provide high-resolution and diffused measurements/information. In this study, moving from videos of a vibrating structure, its dynamic response is assessed. By means of a phase-based optical flow methodology, a linear correlation between the phase and the structural motion is customarily assumed by e.g., the Gabor filter. Since such a correlation does not result to be always linear, a linearization is necessary for all the frames. By using the blind source separation method, mode shapes and vibration frequencies are finally obtained. The performance of the proposed method is investigated, to testify the accuracy in extracting the dynamic features of the considered structure.

**Keywords:** structural health monitoring; modal analysis; blind source separation method; Gabor filter; optical flow

**Citation:** Azizi, S.; Karami, K.; Mariani, S. Vision-Based Structural Identification Using an Enhanced Phase-Based Method. *Eng. Proc.* **2023**, *56*, x. <https://doi.org/10.3390/xxxxx>

Academic Editor(s): Name

Published: 15 November 2023



**Copyright:** © 2023 by the authors. Submitted for possible open access publication under the terms and conditions of the Creative Commons Attribution (CC BY) license (<https://creativecommons.org/licenses/by/4.0/>).

## 1. Introduction

Modal analysis is a vital tool to identify the dynamic behavior of structures in terms of natural frequencies, mode shapes, and damping ratios [1–3]. By understanding how the structures respond to the external forces, it can be ensured that they withstand such loads and also the environmental conditions [4]. Modal analysis serves as a crucial tool in model order reduction techniques [5,6], and structural health monitoring (SHM) [7]. In recent times, vision-based measurements have emerged as a highly effective method for full-field identification [8,9], damage detection [10], model updating [11], and response measurement [12,13]. This innovative approach exploits the data from images to gain insights into the structural behavior. Further than the high-resolution response measurement, it prevents the additional weight linked to the sensing system, and the cost of purchasing, installing, and maintaining sensors.

Optical flow estimation is a method in computer vision that tracks the movement of pixels between consecutive frames of a video. Fleet and Jepson [14] demonstrated that the local phase of an image, obtained through quadratic filters [15], represents motion more robustly than the intensity. Phase-based motion magnification introduced by Wadhwa et

al. [16] involves the amplification of subtle motions in a video sequence, by focusing on the phase information. By means of this technique, Yang et al. [17] obtained the mode shapes from videos of vibrating structures. These mode shapes were subsequently employed in [18] to identify and locate damage, see also [19]. Southwick et al. [20] expanded this approach to extract 3D volumetric motions. Lou et al. [21] introduce a novel image processing technique that addresses the challenge of vision sensors for outdoor structural displacement monitoring, as the conventional approach is susceptible to noise and limited in the measurement range. To enhance the accuracy, Cai et al. [22] addressed the limitations of phase-based estimation and proposed a novel multi-view measurement method. Miao et al. [23], by optimizing the Gabor filter parameters introduced a robust phase-based displacement measurement technique to capture vibration responses.

In this paper, we explore the impact of a specific filter parameter on the filtering response. As it results crucial to recognize that not all the pixels in an image are suitable for motion detection or identification processes, the selection of the appropriate one(s) is a critical concern. Via a defined criterion, regions are identified where the linear correlation between phase and motion is not established. This detection process enhances the accuracy of motion estimation. The phase-based displacement measurement is applied to a real case test, and phase-based identification, incorporating Independent Component Analysis (ICA) blind source separation, is performed on videos of a vibrating structure.

## 2. Motion and Phase Relation

In one-dimensional signal analysis, phase delay is related to how signals evolve over time; the same concept can be applied to two-dimensional signals like images. When a feature in an image undergoes spatial movement, like a translation or a rotation, it leads to changes in the local phase of pixels. This shift in phase is directly related to the extent and direction of the movement.

Fleet and Jepson [14] explored the connection between local phase difference and motion. By tracking the constant phase contours in successive frames, a motion field can be obtained. By assuming that the intensity of the first frame at time  $t_0$  at a pixel with coordinate  $X(x,y)$  is  $I(X)$ , if it gets displaced by  $\Delta(X,t)$  the intensity profile of the next frame at time  $t_1$  is  $I(X + \Delta(X,t))$ . To extract the local phase, it is necessary to use filters like the Gabor one.

The response of the Gabor filter is a complex valued function that can be expressed as:

$$R(X, t) = \rho(X, t) \times e^{i\phi(X, t)} \quad (1)$$

where  $\rho(X, t)$  and  $\phi(X, t)$  represents its amplitude and phase component, given by:

$$\begin{aligned} \rho(X, t) &= |R(X, t)| = \sqrt{\text{Re}[R(X, t)]^2 + \text{Im}[R(X, t)]^2} \\ \phi(X, t) &= \arg[R(X, t)] \end{aligned} \quad (2)$$

The tracking of continuous changes in the phase contours over time, provides a reliable approximation of the motion field. In simple terms, points represented by  $X(x, y)$  on these contours maintain a constant value of  $\phi(X, t) = c$ . The displacement in a direction  $\theta$  is then derived from the movement of local phase contours.

## 3. Unreliable Phase Detection

Motion estimation from videos is characterized by a significant challenge: it is not feasible to extract genuine motion data from every pixel. This issue arises due to various factors, including fluctuations in lighting conditions, Gabor filter parameters, varying object scales within the image, and the presence of noise.

To provide an illustration of this problem, Figure 1a displays an image of a chimney located at Politecnico di Milano, as captured using a standard mobile phone camera. Images have then been handled to create a simulated displacement scenario (ten pixels).

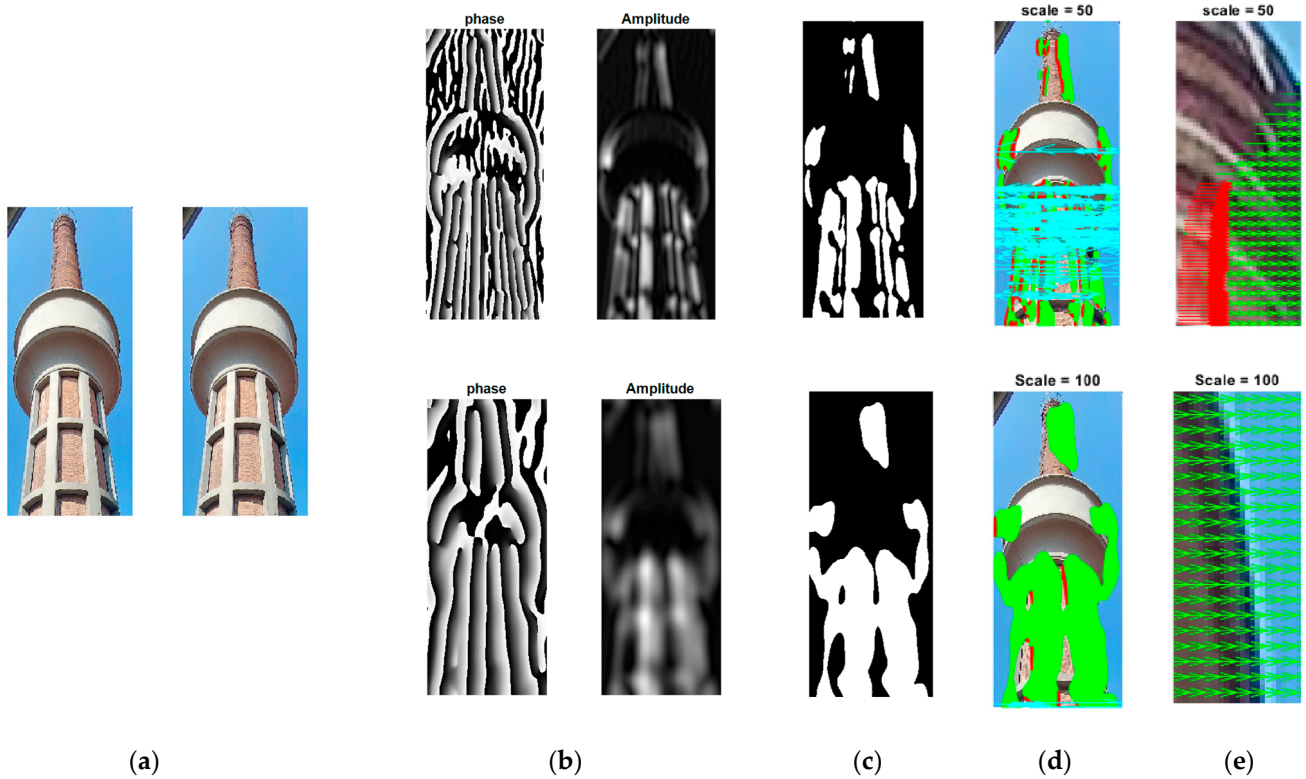


**Figure 1.** (a) Pair of images with 10 pixels displacement between them; (b) contours of amplitude and phase; (c) selected pixel locations; (d) displacement measurement; (e) close-up area. Upper row with scale = 50, lower row with scale = 100.

By Applying the Gabor filter with two different scales, the phase and amplitude are obtained upon suitable pixels are selected for displacement measurement. When the phase varies between  $\pi$  to  $-\pi$  values, jumps (phase wrapping) occurs but should not be considered as an unstable region. A simple way to unwrap the phase is here adopted: when the phase difference between two frames at a point is greater than  $\pi$ ,  $2\pi$  is added or subtracted.

In Figure 1d, displacement measurements with three colors are shown: the green region stands for measurements characterized by an error smaller than 5%, while the red region features measurement errors larger than 5%; the cyan region is instead related to an unstable phase. As shown in the figure, the area representing accurate measurements increases in size at a higher scale, but finer details are lost: for instance, the upper left part of the tower is not captured by the selected pixels at the higher scale.

The phase-based motion estimation methodology is based on the linear correlation between the phase and the structural motion. However, phase nonlinearity stands out as the primary cause of inaccurate motion estimation. By detecting the region in which the phase contours are not likely to provide reliable information about the motion, the measurement error can be reduced. According to [24], two constraints may be needed to detect the points with such a behavior. This approach is here adopted with different bonds on the output of the Gabor filter on an image which is tuned to one scale. A first one is the frequency constraint: the instantaneous frequency of the filter output, which is the spatial gradient of the phase  $\phi_x(X, t)$ , is constrained to be close to the value at which the filter is tuned:

$$|\phi_x(X, t) - k| < \tau \tag{3}$$

A second constraint is instead based on the amplitude: its derivative  $\rho_x(X, t)$  is constrained to be small, according to:

$$|\rho_x(X, t)|/\rho(X, t) < \tau \tag{4}$$

To check the impact of these constraints, the displacement field between two frames of Figure 1a are computed at four scales. Pixels are selected using a simple threshold on the amplitude using Equations (3) and (4). Figure 2 shows that, by employing these thresholds with  $\tau = 0.05$ , cyan regions are completely avoided and the red region is reduced in comparison with that linked to the phase selection solely based on the amplitude.

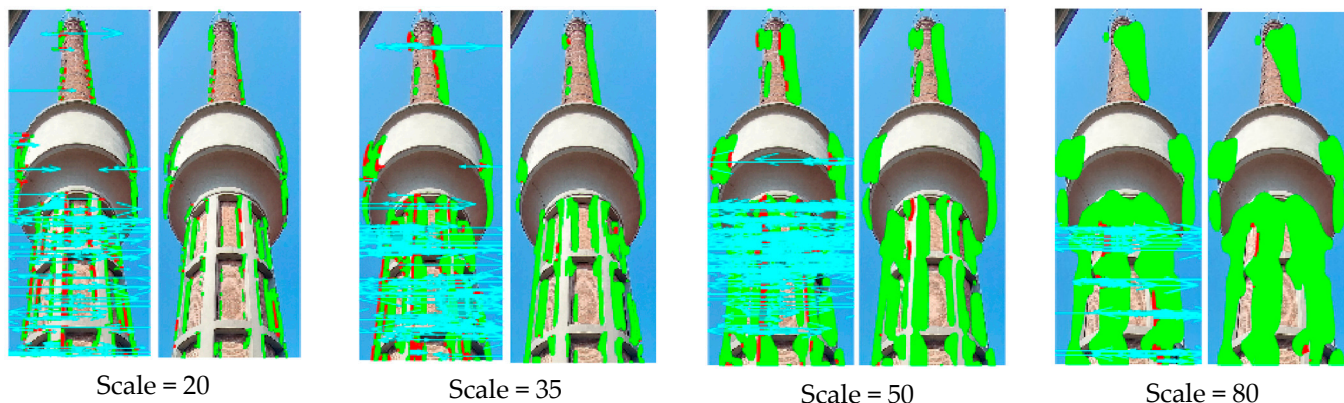


Figure 2. Effect of different thresholds on the displacement measurement between two frames at different scales.

#### 4. Full-Field Identification

An investigation of the performance of pixel selection based on the proposed criteria is now provide, with the aim of identifying full-field modal shapes and vibration frequencies. A model of a ruler subject to free vibrations was captured in a video using MATLAB. Non-linearity in the phase was introduced, to account for a lack of alignment between the filter orientation and the edge of the body. The process of identification is sketched in Figure 3.

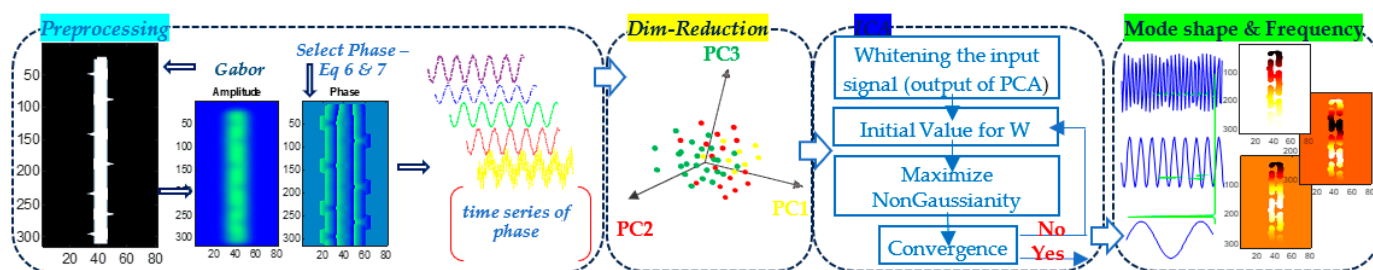
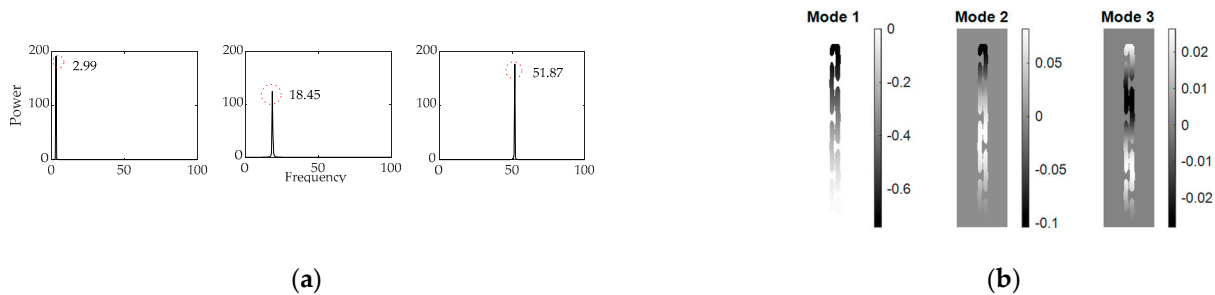


Figure 3. Full-Field identification using PCA-ICA.

By defining the appropriate pixels on the basis of the discussion in Section 3, a matrix is set to represent the time series of selected phases across all frames. By employing PCA, the dimensionality of this matrix is reduced down to the number of excited modes, which turns out to be 3 in the present case. In general cases, the said number of modes is set on the basis of the eigenvalues of the original matrix: to avoid issues related to noise, only principal components linked to eigenvalues larger than 1% of the maximum one are retained in the model. Afterward, by way of ICA [25], the frequencies of vibrations and the corresponding mode shapes are obtained.

In Figure 4a, the identified frequencies (2.99, 18.45, and 51.87) are compared with their corresponding real values (2.93, 18.63, and 51.77), to prove a remarkable accuracy

amounting to 98%, 99.04%, and 99.8% respectively. Figure 4b shows the identified mode shapes, which are compared to the real ones using the modal assurance criterion, revealing similarities of 99.1%, 96.7%, and 98.2% respectively. In Figure 5, it is further demonstrated that the selected regions all have consistent representations of the mode shapes.



**Figure 4.** Identified (a) vibration frequencies, and (b) mode shapes.

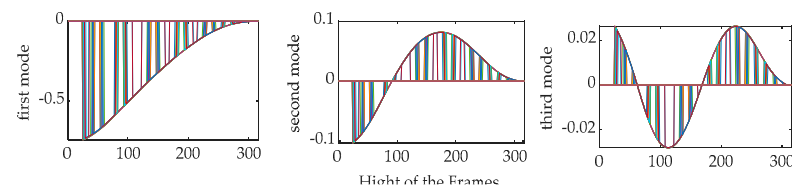


**Figure 5.** First, Second and Third Identified Mode shapes.

## 5. Conclusions

In this study, the impact of the bandwidth of the Gabor filter on the phase extracted from images of a video of structural vibrations, has been investigated. By enlarging the value of this parameter, the level of details under examination is decreased; instead, by decreasing it the linear relationship assumption between phase and motion gets violated. Choosing appropriate pixels for the analysis therefore poses challenges in image processing. By imposing specific conditions on the phase and amplitude of the filtered images, artificial displacement in a real structure has been examined. It has been observed that these conditions have allowed identification of unsuitable phase areas, to get more accurate solutions. Moreover, the selected phases have been exploited for blind modal identification, after dimensionality reduction through PCA and application of ICA. The identified frequencies and modal shapes have been shown to match well the real ones.

In this investigation, pixel selection has been determined exclusively using the first frame of the video. However, considering the potential effects of non-linearity, this choice might differ across different frames. The objective in future research is to identify these locations across all frames, remove them, and subsequently provide accurate estimations using learning-based methods.

## Reference

1. Rosafalco, L.; Eftekhari Azam, S.; Manzonei, A.; Corigliano, A.; Mariani, S. Unscented Kalman Filter Empowered by Bayesian Model Evidence for System Identification in Structural Dynamics. *Comput. Sci. Math. Forum.* **2022**, *2*, 3.
2. Azizi, S.; Karami, K.; Nagarajaiah, S. Developing a semi-active adjustable stiffness device using integrated damage tracking and adaptive stiffness mechanism. *Eng. Struct.* **2021**, *238*, 112036. <https://doi.org/10.1016/j.engstruct.2021.112036>.
3. Amini, F.; Karami, K. Damage detection algorithm based on identified system Markov parameters (DDA/ISMP) in building structures with limited sensors. *Smart Mater. Struct.* **2012**, *21*, 055010. <https://doi.org/10.1088/0964-1726/21/5/055010>.
4. Gatti, F.; Rosafalco, L.; Colombera, G.; Mariani, S.; Corigliano, A. Multi-storey shear type buildings under earthquake loading: Adversarial learning-based prediction of the transient dynamics and damage classification. *Soil Dyn. Earthq. Eng.* **2023**, *173*, 108141. <https://doi.org/10.1016/j.soildyn.2023.108141>.

5. Torzoni, M.; Rosafalco, L.; Manzoni, A.; Mariani, S.; Corigliano, A. SHM under varying environmental conditions: An approach based on model order reduction and deep learning. *Comput. Struct.* **2022**, *266*, 106790. <https://doi.org/10.1016/j.compstruc.2022.106790>.
6. Rosafalco, L.; Manzoni, A.; Mariani, S.; Corigliano, A. Combined model order reduction techniques and artificial neural network for data assimilation and damage detection in structures. In *Computational Sciences and Artificial Intelligence in Industry: New Digital Technologies for Solving Future Societal and Economical Challenges*; 2022; pp. 247–259.
7. Torzoni, M.; Manzoni, A.; Mariani, S. Structural health monitoring of civil structures: A diagnostic framework powered by deep metric learning. *Comput. Struct.* **2022**, *271*, 106858. <https://doi.org/10.1016/j.compstruc.2022.106858>.
8. Feng, D.; Feng, M.Q. Experimental validation of cost-effective vision-based structural health monitoring. *Mech. Syst. Signal Process.* **2017**, *88*, 199–211. <https://doi.org/10.1016/j.ymsp.2016.11.021>.
9. Yang, Y.; Dorn, C. Affinity propagation clustering of full-field, high-spatial-dimensional measurements for robust output-only modal identification: A proof-of-concept study. *J. Sound Vib.* **2020**, *483*, 115473. <https://doi.org/10.1016/j.jsv.2020.115473>.
10. Dworakowski, Z.; Kohut, P.; Gallina, A.; Holak, K.; Uhl, T. Vision-based algorithms for damage detection and localization in structural health monitoring. *Struct. Control Health Monit.* **2016**, *23*, 35–50. <https://doi.org/10.1002/stc.1755>.
11. Martini, A.; Tronci, E.M.; Feng, M.Q.; Leung, R.Y. A computer vision-based method for bridge model updating using displacement influence lines. *Eng. Struct.* **2022**, *259*, 114129. <https://doi.org/10.1016/j.engstruct.2022.114129>.
12. Yang, Y.; Jung, H.; Dorn, C.; Park, G.; Farrar, C.; Mascareñas, D. Estimation of full-field, full-order experimental modal model of cable vibration from digital video measurements with physics-guided unsupervised machine learning and computer vision. *Struct. Control Health Monit.* **2019**, *26*, e2358.
13. Bhowmick, S.; Nagarajaiah, S.; Lai, Z. Measurement of full-field displacement time history of a vibrating continuous edge from video. *Mech. Syst. Signal Process.* **2020**, *144*, 106847. <https://doi.org/10.1016/j.ymsp.2020.106847>.
14. Fleet, D.J.; Jepson, A.D. Computation of component image velocity from local phase information. *Int. J. Comput. Vis.* **1990**, *5*, 77–104. <https://doi.org/10.1007/bf00056772>.
15. Weldon, T.P.; Higgins, W.E.; Dunn, D.F. Efficient Gabor filter design for texture segmentation. *Pattern Recognit.* **1996**, *29*, 2005–2015. [https://doi.org/10.1016/s0031-3203\(96\)00047-7](https://doi.org/10.1016/s0031-3203(96)00047-7).
16. Wadhwa, N.; Rubinstein, M.; Durand, F.; Freeman, W.T. Phase-based video motion processing. *ACM Trans. Graph.* **2013**, *32*, 1–10. <https://doi.org/10.1145/2461912.2461966>.
17. Yang, Y.; Dorn, C.; Mancini, T.; Talken, Z.; Kenyon, G.; Farrar, C.; Mascareñas, D. Blind identification of full-field vibration modes from video measurements with phase-based video motion magnification. *Mech. Syst. Signal Process.* **2017**, *85*, 567–590.
18. Yang, Y.; Dorn, C.; Mancini, T.; Talken, Z.; Theiler, J.; Kenyon, G.; Farrar, C.; Mascareñas, D. Reference-free detection of minute, non-visible, damage using full-field, high-resolution mode shapes output-only identified from digital videos of structures. *Struct. Health Monit.* **2018**, *17*, 514–531.
19. Yang, Y.; Jung, H.; Dorn, C.; Park, G.; Farrar, C.; Mascareñas, D. Estimation of full-field dynamic strains from digital video measurements of output-only beam structures by video motion processing and modal superposition. *Struct. Control Health Monit.* **2019**, *26*, e2408.
20. Southwick, M.; Mao, Z.; Niezrecki, C. Volumetric Motion Magnification: Subtle Motion Extraction from 4D Data. *Measurement* **2021**, *176*, 109211. <https://doi.org/10.1016/j.measurement.2021.109211>.
21. Luo, L.; Feng, M.Q.; Wu, Z.Y. Robust vision sensor for multi-point displacement monitoring of bridges in the field. *Eng. Struct.* **2018**, *163*, 255–266. <https://doi.org/10.1016/j.engstruct.2018.02.014>.
22. Cai, E.; Zhang, Y.; Ji, X.; Lu, X.; Xie, L.; Zhuang, Y.; Zhao, T.; Lin, G. Estimating small structural motions from multi-view video measurement. *Eng. Struct.* **2023**, *275*, 115259. <https://doi.org/10.1016/j.engstruct.2022.115259>.
23. Miao, Y.; Jeon, J.Y.; Kong, Y.; Park, G. Phase-based displacement measurement on a straight edge using an optimal complex Gabor filter. *Mech. Syst. Signal Process.* **2021**, *164*, 108224. <https://doi.org/10.1016/j.ymsp.2021.108224>.
24. Jepson, A.D.; Fleet, D.J. Phase singularities in scale-space. *Image Vis. Comput.* **1991**, *9*, 338–343. [https://doi.org/10.1016/0262-8856\(91\)90039-r](https://doi.org/10.1016/0262-8856(91)90039-r).
25. Hyvärinen, A.; Oja, E. Independent component analysis: Algorithms and applications. *Neural Netw.* **2000**, *13*, 411–430. [https://doi.org/10.1016/s0893-6080\(00\)00026-5](https://doi.org/10.1016/s0893-6080(00)00026-5).

**Disclaimer/Publisher’s Note:** The statements, opinions and data contained in all publications are solely those of the individual author(s) and contributor(s) and not of MDPI and/or the editor(s). MDPI and/or the editor(s) disclaim responsibility for any injury to people or property resulting from any ideas, methods, instructions or products referred to in the content.